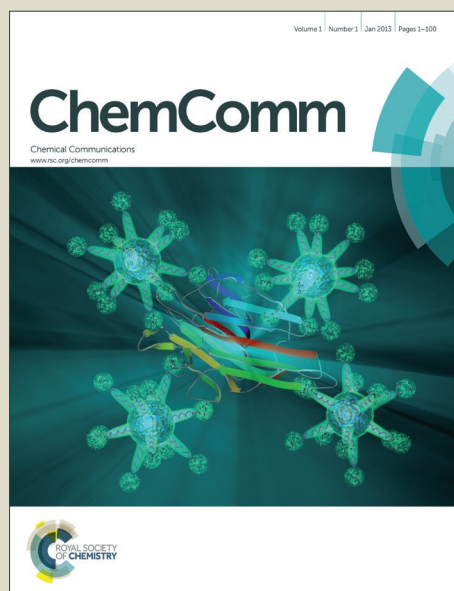


# ChemComm

Accepted Manuscript



This is an *Accepted Manuscript*, which has been through the Royal Society of Chemistry peer review process and has been accepted for publication.

*Accepted Manuscripts* are published online shortly after acceptance, before technical editing, formatting and proof reading. Using this free service, authors can make their results available to the community, in citable form, before we publish the edited article. We will replace this *Accepted Manuscript* with the edited and formatted *Advance Article* as soon as it is available.

You can find more information about *Accepted Manuscripts* in the [Information for Authors](#).

Please note that technical editing may introduce minor changes to the text and/or graphics, which may alter content. The journal's standard [Terms & Conditions](#) and the [Ethical guidelines](#) still apply. In no event shall the Royal Society of Chemistry be held responsible for any errors or omissions in this *Accepted Manuscript* or any consequences arising from the use of any information it contains.

## COMMUNICATION

# Biodegradable Hollow Silica Nanospheres Containing Gold Nanoparticle Arrays

Cite this: DOI: 10.1039/x0xx00000x

Domenico Cassano,<sup>a,b</sup> Diego Rota Martir,<sup>a</sup> Giovanni Signore,<sup>a</sup> Vincenzo Piazza,<sup>a</sup> and Valerio Voliani<sup>\*:a</sup>

Received 00th January 2012,

Accepted 00th January 2012

DOI: 10.1039/x0xx00000x

www.rsc.org/

**We introduce biodegradable hollow silica nanocapsules embedding arrays of 3 nm gold nanoparticles. The silica shell degrades in full serum in few hours, potentially allowing the clearance of the capsules and their contents by the efficient renal pathway, and therefore overcoming accumulation issues typical of metal nanoparticles.**

The huge promise of the application of engineered nanoparticles for theranostics stems from the possibility to design their geometry and surface coating to achieve peculiar chemical, physical and physiological features, allowing simultaneous targeting, diagnostic, and/or therapeutic functionality, potentially tailored for a specific patient or disease.<sup>1,2</sup> Notably, the average diameter of most of the metal inorganic nanoparticles – which shown an enormous potential for the therapy and/or diagnosis of a number of cancers<sup>3</sup> – proposed for *in vivo* theranostics is over 20 nm.<sup>4,5</sup> Unluckily, excretion of objects above 10 nm occurs through liver and spleen into bile and feces but the excretion of intact metal nanoparticles from these pathways is an extremely slow and inefficient process, leading to unwanted accumulation which in turns causes increased toxicity and interference with common medical diagnosis.<sup>6,7</sup> US Food and Drug Administration requires that agents injected into the human body, especially diagnostic agents, are cleared completely in a reasonable amount of time, avoiding persistence in the organism;<sup>6</sup> this requisite is currently not fulfilled by any metal based nanoparticle.<sup>4</sup>

On the other hand, nanoparticles with a diameter of few nanometers would show ideally-fast clearance kinetics through renal excretion, which is controlled by glomerular filtration and shows a threshold of maximum 6 nm,<sup>1,6,8,9</sup> though it should be noted that excessively fast

clearance could hamper some therapeutic applications.<sup>10,11</sup> Yet, the physical and chemical properties of metallic nanoparticles strongly depend on their size and the promise shown by particles above 20 nm size range are usually lost or altered when they are made smaller.<sup>11</sup> Overall, the dilemma concerning the optimal particle size for clinical applications is still unresolved,<sup>1</sup> and only few suggestions were proposed that partially address the issue.<sup>10,12</sup>

Here, we present a modular system that combines the optical behavior of metal nanoparticles with a potentially complete body clearance. Our proposed structure is composed of three elements: 1) small gold nanoparticles (diameter: 3 nm), 2) commercial polymers surrounding the gold nanoparticles; 3) a degradable silica shell embedding the polymer-nanoparticle assembly. Interestingly, the degradation products of these nanomaterials are the polymers, small gold nanoparticles and silicic acid,<sup>13</sup> compatible with the possibility to overcome accumulation owing to the renal clearance of these building blocks.

The general synthetic approach employed for the preparation of hollow silica nanospheres containing the gold nanoparticles array (AuSi) is shown in Figure 1A. Gold nanoparticles of  $2.8 \pm 0.4$  nm (Figure 1B) coated by negative poly(sodium 4-styrene sulfonate) (PSS) were aggregated in spherical arrays by the positive poly(D- or L-lysine) (PL) by means of ionic interactions, and then the silica shell was grown on this template by a modified Stöber method.<sup>13</sup> We suggest that the hollow silica nanosphere formation around the gold array is linked to the presence in the same gold aggregate of both amines from PL and aromatic moieties from PSS. Indeed it was demonstrated that PL alone can be used as template by resulting in hollow silica microspheres only in presence of aromatic additives.<sup>14</sup>

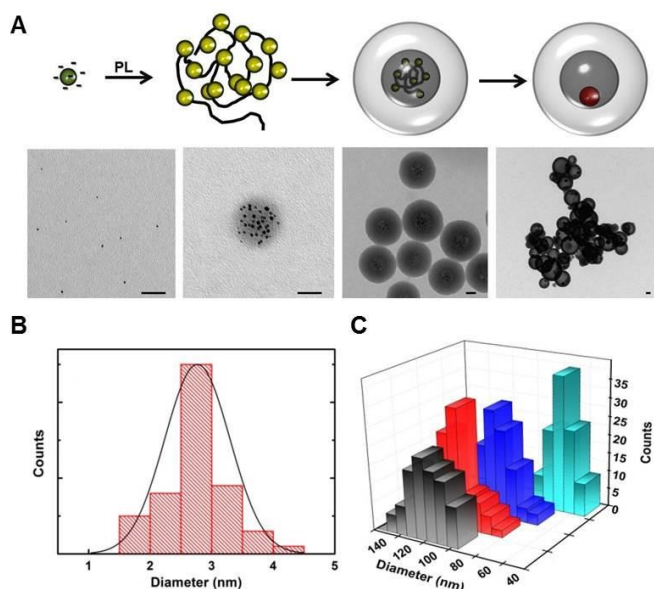


**Figure 1.** A) Top panel: scheme for the general formation of the nanosystem. Negative gold nanoparticles are assembled in spherical arrays employing poly(L-lysine) or dye-modified poly(L-lysine). These cores are then embedded in hollow silica shells. After calcination the organic compounds are burned and the silica shell remained intact, while gold nanoparticles are melted in a single bigger gold nanoparticle presenting a “naked” surface. Bottom panel: TEM images of each synthetic step. Scalebars 25 nm. B) Size distribution histograms of gold nanoparticles. C) Size distribution histograms of AuSi made by employing poly(L-lysine) of various molecular weight: AuSi1 (1-5 kDa) in turquoise, AuSi2 (4-15 kDa) in blue, AuSi3 (15-30 kDa) in red and AuSi4 (70-150 kDa) in black. All the histograms were made on diameter measurements of at least 100 nanoparticles observed by TEM.

For consistence of the work, all the reported results are related to AuSi systems synthesized using poly(L-lysine). TEM images at different tilted angles (Supporting Information Figure S1) and SEM images (Supporting Information Figure S2) confirmed the presence of gold nanoparticles only inside the cavity of silica nanospheres and not entrapped in the wall or on the external surface of the structures.

The hollow silica nanospheres are formed around the gold arrays, which are used as templates. Thus, a good control over the size of gold aggregates is required in order to obtain AuSi with a size in the nanometer range.<sup>14</sup> This was achieved by employing during the array formation an optimized weight ratio between gold nanoparticles and PL (see Supporting Information), which decreases the possibility to have large aggregates (Supporting Information Figure S3). Also, in order to test if the size of AuSi was related to the molecular weight of the PL used for the array formation (Figure 1C), various PLs were employed: PL 1-5 kDa was used to synthesize AuSi1 systems, while PL 4-15 kDa for AuSi2, PL 15-30 kDa for AuSi3 and PL 70-150 kDa for AuSi4, yielding nanosystems with diameters of:  $59 \pm 8$  nm,  $93 \pm 11$  nm,  $108 \pm 12$  nm, and  $110 \pm 13$  nm respectively. Apparently, there is no strict relation between diameters of AuSi1-4 and polymerization degree of PLs.<sup>14</sup> This trend can be probably ascribed to the purification protocol employed, in which the colloids are subjected to a short centrifugation step after the reactions in order to remove the larger particles (see Supporting Information).

Keeping in mind that physiological effects such as the Enhanced Permeability and Retention (EPR) are optimally addressed as a viable

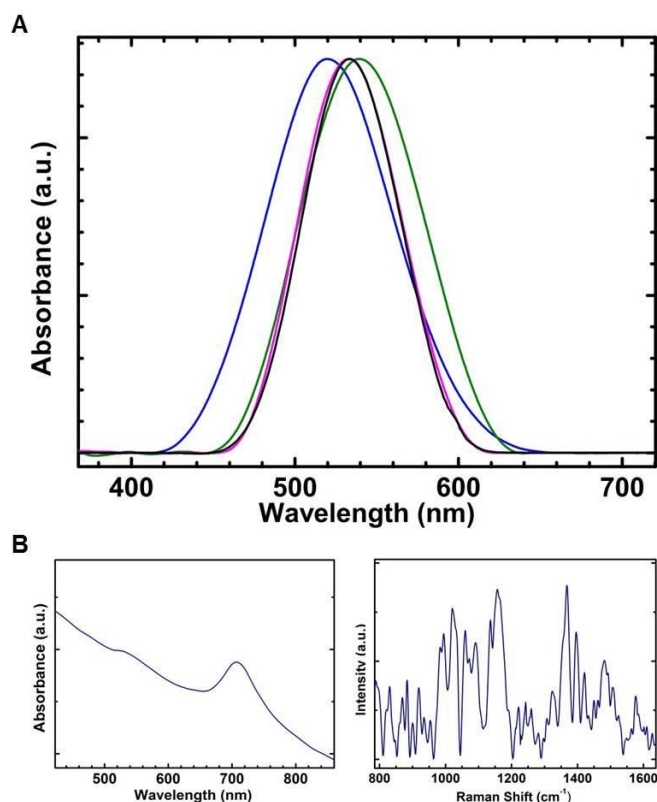


**Figure 2.** A) Spectral behavior of 3 nm gold nanoparticles (blue), gold arrays (green), AuSi3 (purple), and calcinated AuSi3 (black). Spectra were collected in milliQ water, normalized and the background subtracted. B) Absorbance (left) and SERS (right, background subtracted) spectra of AuSi3A collected, respectively, in ethanol and milliQ water.

theranostics pathway by particles sized around 100 nm,<sup>1</sup> we focused on the synthesis of AuSi3. The optical behavior of the latter and of its components is reported in Figure 2A. The extinction band of the mother solution of gold nanostructures is below 520 nm. As expected, the band shifts to red (at 539 nm) after the aggregation with PL, owing to the close proximity of the nanoparticles in the array. When gold arrays are included in the hollow silica nanospheres the extinction band experiences a minor blue-shift to 532 nm, likely due to increased purity and more homogeneous size of the processed nanostructures (see Supporting Information). This demonstrates that gold nanoparticles in AuSi3 are actually kept strictly packed in a spherical shape by PL, showing optical behavior that could promote typical diagnostic/therapeutic applications of metal nanoparticles.<sup>25,26</sup> Notably, we observed that upon calcination, the polymers in the AuSi cavity are degraded and gold nanoparticles melt forming a single gold structure (see Supporting Information Figures S4-5) whose optical behavior is similar to AuSi3.

An interesting aspect of AuSi nanocapsules stems from the possibility of incorporating other functional motifs inside their core, such as drugs or magnetic elements for the production of multimodal systems. To test this feature, PL 15-30 kDa was modified with AlexaFluor-680 NHS ester and used to synthesize the gold arrays and then the AuSi3A system. The absorbance spectrum of AuSi3A is reported in Figure 2B (left panel), where both bands of gold array and of the dye are present. SERS experiments were performed (Figure 2B

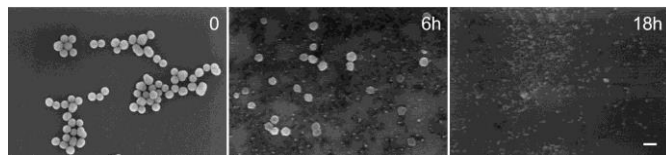


**Figure 3.** A) SEM images of AuSi<sub>3</sub> after incubation in full serum at 37 °C. Scalebars: 200 nm.

right panel) in order to confirm the presence of the fluorophore in the cavity of AuSi<sub>3</sub>A and near the gold nanoparticles surface. The SERS signals were compared and consistent with the Raman shifts achieved from milliQ water solution of AlexaFluor-680 (Supporting Information Figure S6) demonstrating that the modification of PL does not affect its solvating properties over gold nanoparticles and thus the success of the reaction. It is also noticeable that: i) the surface of these highly reproducible systems is modifiable by functional coatings with standard protocols (Supporting Information Figure S7), and ii) they can be subjected to freeze-drying and stored for up to one year without losing their properties.

We also evaluated degradation kinetics of our nanostructures in physiological media, comparing our results with similar findings obtained with silica nanoparticles.<sup>33</sup> We performed SEM imaging experiments of AuSi<sub>3</sub> incubated in full serum at 37 °C (Figure 3). After six hours the nanosystems lose their spherical shape appearing eroded, while after 18 hours no more nanoparticles were observed in the samples. Note that the maximum silicic acid solubility can exceed the equilibrium saturation concentration (see Supporting Information) causing a condensation via Ostwald ripening effect and forming the background material on the silicon wafer.<sup>33</sup>

Overall, it can be envisioned that the proposed nanosystem: i) reaches the target in the organism, ii) exploits its therapeutic/diagnostic action, iii) biodegrades in the building blocks and the latter are excreted. It is also reasonable to expect that the released gold nanoparticles be completely coated by endogenous glutathione before the renal clearance, decreasing their possible adverse effect.<sup>37</sup>

## Conclusions

In summary we have presented a highly reproducible, functional and biodegradable nanosystem composed by hollow silica nanoparticles in which 3 nm gold nanoparticles are embedded in their central cavity in a narrow array, able to simulate the optical behaviour of a single larger gold nanoparticle. Noticeably, these nanosystems stand as promising tools to overcome the issue of accumulation of inorganic nanoparticles in organisms. Preliminary *in vivo* photoacoustic and x-ray experiments are ongoing. Also, the possibilities to develop gold arrays with peculiar geometries (and thus peculiar optical behaviour, such as rods) and nanosystems devoid of metal nanoparticles are under investigation. Finally, their calcination produces "naked" gold nanoparticles – i.e. without any type of coating on the surface - shielded by the hollow permeable silica nanospheres. These nanosystems could be very performing as catalysers over a number of reactions, among which the water-gas shift reaction. This task will be also supported by the versatility of the nanosystems, i.e. the possibility to synthesize nanostructures composed by various metals, among which platinum and silver.

## Acknowledgement

We would like to thank Dr. Camilla Coletti and Mrs. Domenica Convertino for fruitful discussion and the Renishaw Raman Microscope and furnace facilities. We would also like to thank Dr. Mauro Gemmi for his help in TEM imaging, Dr. Stefano Luin for SERS facilities, and Prof. Fabio Beltram for fruitful discussion.

## Notes and references

<sup>a</sup> Center for Nanotechnology Innovation @NEST, Istituto Italiano di Tecnologia, P.zza San Silvestro, 12 - 56126, Pisa (PI), Italy. Mail: [valerio.voliani@iit.it](mailto:valerio.voliani@iit.it)

<sup>b</sup> NEST-Scuola Normale Superiore, P.zza San Silvestro, 12 - 56126, Pisa (PI), Italy.

† Electronic Supplementary Information (ESI) available: experimental details, SEM/TEM images and SERS spectra. See DOI: 10.1039/c000000x/

1. T. Sun, Y. S. Zhang, B. Pang, D. C. Hyun, M. Yang, and Y. Xia, *Angew. Chemie Int. Ed.*, 2014, **53**, 12320–12364.
2. V. Voliani, F. Ricci, S. Luin, and F. Beltram, *J. Mater. Chem.*, 2012, **22**, 14487.
3. E. C. E. Dreaden, A. A. M. Alkilany, X. Huang, C. J. Murphy, and M. a El-Sayed, *Chem. Soc. Rev.*, 2011, **41**, 2740–2779.
4. M. L. Etheridge, S. a Campbell, A. G. Erdman, C. L. Haynes, S. M. Wolf, and J. McCullough, *Nanomedicine*, 2013, **9**, 1–14.
5. V. Voliani, G. Signore, O. Vittorio, P. Faraci, S. Luin, J. Pérez-, J. Pérez-Prieto, and F. Beltram, *J. Mater. Chem. B*, 2013, **1**, 4225.
6. H. S. Choi, W. Liu, P. Misra, E. Tanaka, J. P. Zimmer, B. Itty Ipe, M. G. Bawendi, and J. V Frangioni, *Nat. Biotechnol.*, 2007, **25**, 1165–70.
7. S. M. Moghimi, A. C. Hunter, and J. C. Murray, *Pharmacol. Rev.*, 2001, **53**, 283–318.
8. C. Zhou, M. Long, Y. Qin, X. Sun, and J. Zheng, *Angew. Chem. Int. Ed. Engl.*, 2011, **50**, 3168–72.
9. X.-D. Zhang, D. Wu, X. Shen, P.-X. Liu, F.-Y. Fan, and S.-J. Fan, *Biomaterials*, 2012, **33**, 4628–38.
10. J. M. Tam, J. O. Tam, A. Murthy, D. R. Ingram, L. L. Ma, K. Travis, K. P. Johnston, and K. V Sokolov, *ACS Nano*, 2010, **4**, 2718.
11. L.-Y. Chen, C.-W. Wang, Z. Yuan, and H.-T. Chang, *Anal. Chem.*, 2015, **87**, 216–29.
12. A. Samanta, B. B. Dhar, and R. N. Devi, *J. Phys. Chem. C*, 2012, **116**, 1748–1754.
13. E. Mahon, D. R. Hristov, and K. a Dawson, *Chem. Commun. (Camb.)*, 2012, **48**, 7970–2.
14. K. Van Bommel, J. Jung, and S. Shinkai, *Adv. Mater.*, 2001, **13**, 1472–1476.
15. J. R. Cook, W. Frey, and S. Emelianov, *ACS Nano*, 2013, **7**, 1272–1280.
16. J. F. Hainfeld, F. A. Dilmanian, D. N. Slatkin, and H. M. Smilowitz, *J. Pharm. Pharmacol.*, 2008, **60**, 977–985.
17. J. Liu, M. Yu, C. Zhou, S. Yang, X. Ning, and J. Zheng, *J. Am. Chem. Soc.*, 2013, **135**, 4978–4981.